THE JOURNAL OF PHYSICAL CHEMISTRY B

Article

pubs.acs.org/JPCB

Unravelling the Structure of Protic Ionic Liquids with Theoretical and Experimental Methods: Ethyl-, Propyl- and Butylammonium Nitrate Explored by Raman Spectroscopy and DFT Calculations

E. Bodo,*[,†,∥] S. Mangialardo,[‡] F. Ramondo,[§] F. Ceccacci,[†] and P. Postorino[‡]

[†]Department of Chemistry and [‡]Department of Physics, University of Rome "La Sapienza", Italy

[§]Department of Chemistry, Chemical Engineering and Materials, University of L'Aquila, via Vetoio, Coppito, I 67100 L'Aquila, Italy

ABSTRACT: We present an analysis of gas-phase structures of small clusters of *n*-alkylammonium nitrates (ethyl, propyl, and butyl) together with vibrational Raman spectroscopy of their respective liquid phases. The assignment and interpretation of the resonant frequencies have been performed by comparison with high-quality ab initio (DFT) computations. The theoretical spectra are in excellent agreement with the measured ones and allow the interpretation and assignment of almost all the spectral features. A careful analysis of the vibrational frequencies and of the electronic structure of the compounds has provided additional information on various structural features and on the rather complex hydrogen bonding network that exists in such compounds. A geometric structure of the short-range local arrangement in the bulk phases is also proposed.

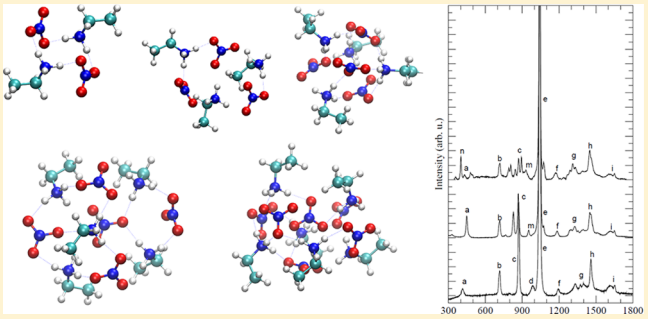

INTRODUCTION

Ionic liquids,[1−4] in the past decade, have attracted a great deal of attention among the new materials because they can certainly claim one of the most rich field of applications in industry and in applied technologies. Their long story, tightly connected to the molten salts research field, dates back to 1914 with the synthesis of ethylammonium nitrate by Walden[5] and, in more recent times, has seen an extraordinary parallel development between academic research and industrial applications.[6] Although many studies, both theoretical and experimental, are nowadays devoted to understand their behavior, these substances still lack a coherent and general theoretical framework able to describe their complex properties.[7−9]

These substances contain an organic cation (e.g., an asymmetric derivative of the 1-alkylpyridinium, tetraalkylphosphonium, 1,3-dialkylimidazolium or tetraalkylammonium ions) and an inorganic or organic anion. Their versatility depends on the fact that their properties can be tuned by varying the molecular structure of both the cation and the anion. Thanks to these properties, ionic liquids have soon been recognized[3] as ideal candidates for many and diverse applications. These include their use as a "green"replacement of organic solvents,[7,10] lubricants,[11] ingredients for pharmaceuticals,[12−14] reaction media,[15−18] extraction media in analytical chemistry,[19−21] and solvents for electrochemistry.[22−25]

An appealing subset of ionic liquids are protic ionic liquids (PILs) that can be prepared by combination of Bronsted acids and bases.[26−29] Proton transfer takes place from the acid to the base, leading to the formation of a pure liquid made by ionic couples where proton acceptor and donor sites eventually generate a hydrogen-bonded network.[30] The proton transfer from the base back to the acid rarely takes place in the bulk phase, but it is thought to be the main evaporation mechanism whereby an ionic couple reacts and give rise to a couple of volatile neutral molecules.[31] These features make PILs appealing candidates for new generation fuel cells electrolytes.[32] The presence of a H-bond is of paramount importance for ionic liquids because it can significantly influence a number of phisical properties even if the H-bond is only a significant but small portion of the total interaction energies. In general, the presence of the H-bonds is thought to make these systems more fluid, contrary to what can be seen with conventional molecular liquids.[33] To date, the understanding of PILs performances is very limited, especially in comparison with imidazolium-based moieties. It is well-known that their properties strongly depend on the acid−base equilibrium and, consequently, on temperature. It is remarkable, however, that major issues such as ion−ion interactions, ionic transport, and structural correlations are still far from having been elucidated. Alkylammonium nitrates are among the most studied PILS;[34−38] methylammonium nitrate (MAN) and ethylammonium nitrate (EAN), in particular, are the first ionic liquids ever synthesized.[5]

Only recently have the development of atomistic simulation techniques and the parallel growth of computational power

Received: May 30, 2012
Revised: September 6, 2012
Published: September 13, 2012

   dx.doi.org/10.1021/jp3052714 | *J. Phys. Chem. B* 2012, 116, 13878−13888

reached the point at which it is possible to reliably provide a nanoscopic interpretation of the bulk properties of these materials.[39,40] Atomistic, molecular dynamics (MD) simulations play a crucial role in the ionic liquid research field because they offer the possibility of a rationalization of the experimental observations and because MD is becoming a valuable tool in designing new systems with properties optimized for specific technological applications. MD simulations are bound to the deveopment of suitable force fields[41−44] whose reliability makes them able to interpret the, often, very accurate experimental determinations (e.g., see refs 45 and 46). It is well-known, in fact, that MD simulation techniques are fundamentally based on an empirical modeling of the interaction and that the resulting simulation can provide only a partial interpretation of experimental data. In the past few years, nonempirical, ab initio MD simulations (AIMD) have started to be explored as a tool for assessing ionic liquid bulk properties[47] from "first principles". These simulations, however, are still in their embryonic stage and are limited to very short time scales. To make AIMD doable in a reasonable computational time, the simulated system must only contain a few hundreds atoms and, even in these cases, the simulations have to be run on massively parallel computational facilities. Despite these limitations, AIMD results are encouraging and have been shown to provide unprecedented opportunities[48] and prompt the theoretical chemistry community with the need of additional studies based on first principle description of ionic liquids. In this view we present here a study in which we employ high-quality ab initio structural studies (not dynamical though) to interpret spectroscopic Raman studies of the corresponding bulk liquid systems.

Very recently[49] we have performed a detailed study of the MMAN system in various solid and liquid phases and we have provided a detailed picture of some of the structural features of the system thanks to a joint experimental theoretical effort. In a recent paper Kirchner and co-workers[47] have explored, by means of AIMD simulation, the same compound in its liquid phase. Both studies have confirmed and agree on various structural features: for example, only 1.8−2.0 contacts of the nitrate ion are actually acceptors of strong H-bonds. Therefore, one acceptor and one donor site, on average, remain either free or involved only partially in an H-bond, giving rise to a rather complex and asymmetric H-bonds network. This is extremely important in view of creating/testing a force field framework in which one could obtain a reliable description of the weak interactions at play in these ionic liquids. A recent neutron scattering study on EAN and PAN[37,50] has shown the existence, in these compounds, of structural heterogeneities on a 10 Å scale that are compatible with the existence of alkyl chain aggregation that is the driving force responsible for the formation of micellar aggregates in other structured liquids. This is an additional structural feature that is extremely important, but that is out of the range of the present investigation.

Very recently, an OPLS[51] derived force field has been used in MD simulations to elucidate the low-angle X-ray scattering factors from selected alkylammonium nitrates.[38] We raise some doubts, however, that this model has obtained a complete rendering of the structure of the liquids although it reproduces fairly well most of the X-ray data. One of the most important features of the rather complex H-bonding network is the average H···O distance that the above model finds to be by roughly 2.4 Å, a value that is larger than the value reported by Kirchner[39] and the one that can be calculated ab initio, the latter being below 2.0 Å. The present calculations seem to point in favor of the shorter value which, by the way, seems to be consistent with the typical N−H···O H-bonding features already registered in the literature.[52,53]

METHODS

Raman Measurements. Raman measurements were carried out using a confocal-microscope Raman spectrometer, equipped with a set of interchangeable objectives with long working distances and different magnifications from 4× to 100×. The samples were excited by the 632.8 nm line of a 20 mW HeNe laser. The 1800 lines/mm grating monochromator and a charge-coupled-device (CCD) detector allowed for a spectral resolution better than 3 cm^{-1}. Elastically scattered light was removed by an holographic notch filter, which avoided collection of spectra within the low-frequency spectral region. Raman spectra were indeed collected in backscattering geometry over different spectral ranges spanning from 300 to 3800 cm^{-1}. Using thin quartz cuvettes, we collected the Raman spectra at ambient condition. The use of a rather small confocal diaphragm (<100 μm) allowed us to minimize the contribution arising from the quartz windows.

EAN and PAN were purchased from Iolitech have been dehydrated under a nitrogen flux for 48 h. The BAN compound is not available commercially and therefore was prepared by an adaption of a reported procedure.[54] Solvents (LC-MS grade) and butylamine (99.5%) were purchased from Aldrich. Nitric acid (65% w/w) was purchased from Carlo Erba. The procedure was the following: to a solution of butylamine (2.4 mL, 0.024 mol) in pentane (4 mL) at 20 °C, HNO_3 (65%, 1.2 mL, 0.017 mol) was added dropwise under stirring for 15 min. The reaction was kept at −10 °C for 20 min and then left under stirring for 2 h at room temperature. The pentane layer was separated, the product washed with pentane and dried at the rotary evaporator. Water was removed by keeping the product under high vacuum and efficient stirring at room temperature for 2 days. BAN was obtained as a metastable colorless liquid in 90% yield. The water content, determined by NMR analysis in DMSO-d_6, was below 0.003% wt. Due to its hygroscopic nature, BAN was stored under inert atmosphere.

Geometric Optimization of the Clusters. The calculations have been performed for isolated (gas-phase) small clusters composed of a limited number of ionic couples. A single ionic couple composed of a *n*-alkylammonium nitrate, owing to the nature of the nitrate anion, is unstable toward the formation of the corresponding amine and nitric acid. Starting with two ionic couples, however, the configuration with charge separation becomes more stable than the cluster made by neutral molecules. For example, starting with two molecules of nitric acid interacting with two molecules of and methylamine, the path that leads to the deprotonation of the acids is found to be barrierless and the double proton transfer takes place releasing about 32 kcal.

To maintain the calculations feasible, we have explored only very small clusters composed of a limited number of ionic couples (the quantum calculations reported here are limited to 6 ionic couples, but extensive testing has been performed that included also higher aggregation numbers, without, however, any noticeable change in behavior). A gas-phase optimized cluster represents a very different environment with respect to a room temperature fluid for which the experimental determinations have been done. However, in the case of the present

systems the strength of the ionic interaction makes these differences less marked, especially if compared to situations in which neutral molecules are involved. This is due to the fact that average extraction energy for an ionic couples exceeds 100 kcal.[49] Therefore, we believe that, for these particular systems, the local geometric environment of a small cluster closely resembles the bulk state local arrangement and that the vibrational frequencies determined in the harmonic approximation by optimization techniques can provide a good rendition of the bulk Raman spectra (except for the low-frequency region).

When the number of atoms in a molecular system increases, the number of local minima of the potential energy surface (PES) becomes quickly so large that a systematic search is impossible. In other words, the large number of internal degrees of freedom prevents the exploration of the PES in all the possible geometries of the system. Therefore, one of the main computational problems in the study of the stable geometries of complex molecular systems, especially those characterized by a high conformational mobility such as the ones under study here, is that of locating possible good candidates for the time-consuming, ab initio optimizations. There are many theoretical methodologies that, in an initial stage, bypass the electronic problem and that can help in discovering the lower lying minima over a complex PES for system composed of many atoms: these methods are based on Monte Carlo (MC) sampling,[55] molecular dynamics (MD), or genetic algorithm searches.[56] Here we have used a method based on MC sampling[57] with the OPLS force field[51] (where nitrate Lennard-Jones parameters are taken from ref 58). A scheme of the atom types associated to propylammonium nitrate is reported in Figure 1 along with the naming

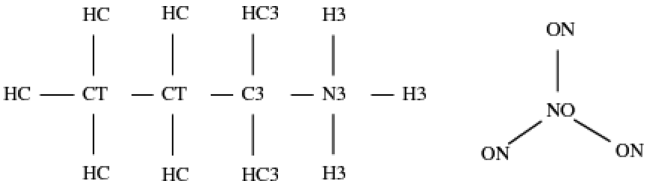

Figure 1. Atom type used in OPLS atomic force field calculations.

conventions in the OPLS force field. The global minima has then been optimized by means of the ab initio DFT method and its infrared (IR) and Raman spectrum in the harmonic approximation has been calculated using the Gaussian program.[59] Generally, the level of the calculation is ωB97X-D/6-311+G(d,p)[60] both in the optimization step and in the normal modes evaluations, but some variations have been done and will be pointed out for specific cases. At the final point (stationary point) we also performed a counterpoise calculation to obtain the "fixed-geometry" binding energies and an NBO analysis using the wB97X functional to obtain the delocalization energy $E(2)$ (see below and ref 61).

Obviously, given the high number of local minima, we cannot be sure whether we are describing the global minima over the potential energy surface of these complexes or only a local one. However, the Monte Carlo procedure mentioned above should be certainly able to produce reasonable structures so that we expect the following ab initio analysis to describe realistically all the key structural features of the complexes. Anyway, because most of the local minima are roughly energetic and structurally equivalent, the chance of having found only a local one should not compromise the normal-mode analysis.

RESULT AND DISCUSSION

Cluster Structures and the H-Bonding Feature. As we did for the MAN compound,[49] we discuss the series of the lowest energy minima we have found for the various chain when increasing the number of ionic couples making the cluster. The lower panel of Figure 2 reports the total classical (force field) energy of the clusters obtained with ethyl, propyl, and butyl alkyl chain lengths. In the upper panel of the same figure we report the backward difference of the total energy, i.e., the evaporation energy or the energy that is needed to extract that particular ionic couple. The trend in the evaporation energy is common to all the three compounds. Beyond a certain size, however, we probably pay the fact that it turns out to be nearly impossible to locate the global minima of the cluster due to its enormous conformational mobility and the data fluctuates beyond n = 10. As can be seen, the average evaporation energy as obtained by the OPLS-based minimizations is around 140 kcal but we can clearly spot a few structures with a more stable configurational energy like 4, 6, and 10. Few selected examples of the classical structures are reported in Figure 3.

The very first terms of the series are interesting because the fluctuations are more marked there. We clearly see the presence of a "magic number" with 4 ionic couples and this is due to the formation of a highly symmetrical configuration made by a cubic cage bound through N−H···O hydrogen bonds. In contrast to what usually happens with atomic or metallic clusters or those composed of small molecules, in the present case, the clusters of these ionic liquids tend to show barely any structural order beyond n = 4. From n = 5 to larger sizes, in fact, the shape of the growing clusters becomes less and less symmetric, as can be seen from the examples reported in Figure 3 for 6 and 10 ionic couples (only EAN6 and EAN10 are shown for the largest clusters). The cubic-like feature noticed before disappears although the alkyl chain tends to remain on the "surface" of the cluster even with many ionic couples. In general, however, we conclude that the cluster becomes much more disordered for a number of ionic couples greater than 6. This is not surprising because the presence of bulky and asymmetric constituent ions is precisely one of the reasons these salts are liquid under ambient conditions. As can be seen, the small clusters tend to show a symmetric structure that is built out of the electrostatic and H-bonding interactions. The distance between H3 and ON in these clusters varies between 1.67 and 1.71 Å. This is somewhat shorter than the 1.8−1.9 Å distances found by ab initio simulations in a similar system[47] or, experimentally, in solid MAN.[49] This difference is simply bound to a deficiency of the OPLS force field: the OPLS Lennard-Jones parameters are optimized on nonionic liquids where no strong electrostatic interaction are found. The OPLS force field therefore tends to overestimate the densities of the ionic liquids in the bulk phase and, in turn, it presents intermolecular distances that are too short in the clusters.

For few selected clusters obtained by the above force field minimization, we have performed a DFT optimization: for EAN we have used the ωB97X-D/6-311+G(d,p) level for the clusters up to 6 ionic couples, whereas for PAN and BAN we have used a ωB97X-D/6-31+G(d) level and we have limited the calculations to the clusters with 4 and 6 ionic couples. For all optimizations we have calculated at the same level the

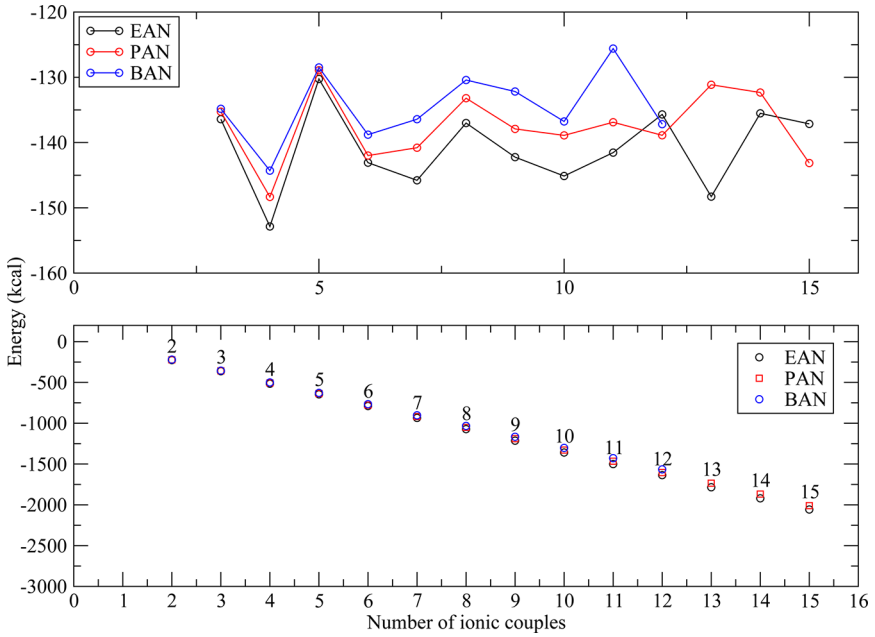

Figure 2. Lower panel: total force field energy for the classical minima by MC minimization as a function of the size of the cluster. Upper panel evaporation energy.

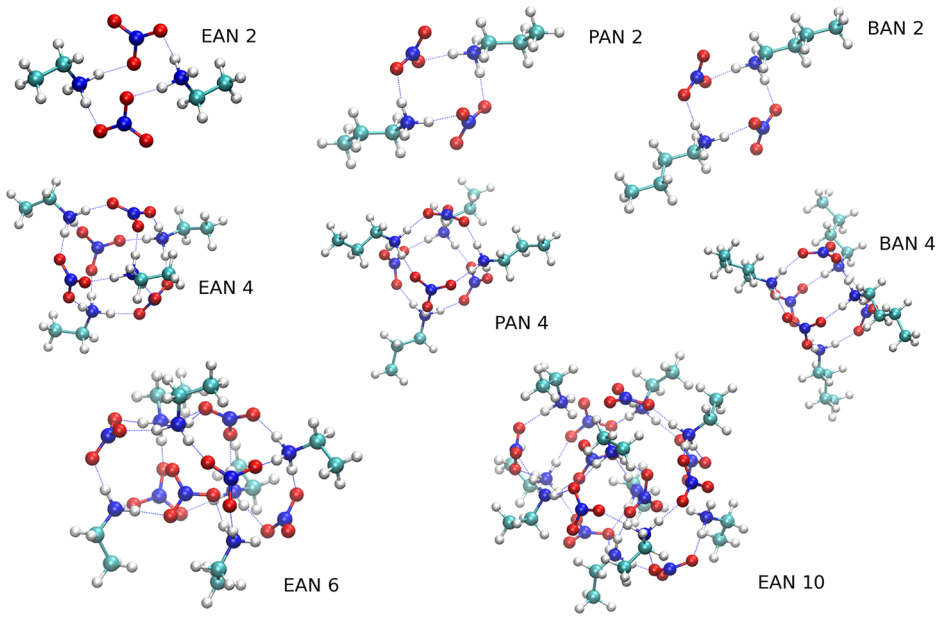

Figure 3. Classically determined minimum energy structures of various compounds.

normal modes of the resulting structures and the corresponding Raman spectrum.

Before examining the resulting quantum structures, we would like to point out the following:

- For EAN and for the cluster corresponding to $n = 2$, we have performed a full geometry optimization using a two-body counterpoise correction to assess the importance of basis set superposition error (BSSE) at that level of calculation. We have noticed that the resulting minima structure is hardly affected by BSSE corrections with structural changes that are within 0.1% of interatomic distances (when compared to the structure obtained with no BSSE correction). The total BSSE energy has been calculated and is around 0.003 au (2 kcal), which is much lower that the typical energetics of the cluster growth as shown above.
- Another test was performed to check to what extent the inclusion of dispersion empirical terms in the ωB97X-D functional were actually important in determining the geometry. We optimized one of the structure using the ωB97X functional, but we noticed very little difference in these systems. In particular, for the EAN system with 3 ionic couples the resulting structures (with and without dispersion corrections) are so similar that the differences account for an rmsd of 0.099 Å (by comparison, the difference between the quantum and classical structures is much larger and generates an rmsd of 2.68 Å). This behavior is rather different from what has been found by

dx.doi.org/10.1021/jp3052714 | J. Phys. Chem. B 2012, 116, 13878−13888

Kirchner and co-workers in ref 62 for the imidazolium moieties where both geometries and energies were much more sensible to the presence of dispersion corrections owing, we believe, to the presence of π electronic systems.

The resulting quantum structures for EAN are reported in Figure 4, but similar ones have been obtained also for PAN and

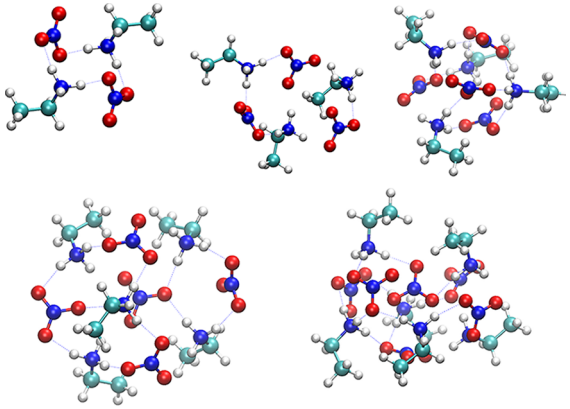

Figure 4. Quantum DFT minimum energy structures of various EAN clusters: clockwise 2, 3, 4, 5, and 6 ionic couples.

BAN. The quantum structures are, on the whole, slightly more disordered than the classical ones. Even for 4 ionic couples, it is difficult to discern patterns reminiscent of the cubic cage structures noticed before. This is probably due to the formation of an H-bonding network that the relatively simple structure of the force field based on Lennard-Jones parameters and point charges (i.e., a force field made of two-body potential energy terms) is unable to reproduce. As can be clearly seen from the quantum structures, the H-bonding is strongly asymmetric: in several anions, one of the O atoms is unable to form a "proper" H-bond. This asymmetry of the NO_3^- anion is difficult to reproduce classically because of the inherent symmetry of the force field types. This asymmetric growth of H-bonds is probably an additional "disordering" factor that makes this ionic liquids actually liquid at room temperature or at mild conditions. This lack of "saturation" of the H-bonding network not only is due to a finite size effect, i.e., to nitrate anions that find themselves on the "surface" of the cluster, but also seems (at least by close inspection of the quantum structures) to affect those located inside the cluster. This "unsaturation" effect, being due to complicated polarization effects, cannot be simply described by a two-body force field that therefore gives rise in the classical optimization to very symmetric structures.

Average distances and angles obtained from the quantum structures are reported in Table 1 where we also report the average distances obtained by a 2 ns classical dynamics on a cluster of 36 ionic couples for comparison. Except for the smallest clusters, the O···H distance is between 1.8 and 1.9 Å, in agreement with what we have found experimentally for the MAN solid phases and with the Car–Parrinello dynamics simulation of Kirchner and co-workers,[47] but substantially different from the value reported in refs 37 and 38 of 2.5 Å. The H-bond angle is between 161 and 166°. Our optimization procedure therefore produces a very typical "bent" H-bond where the donor–acceptor distance is between 2.85 and 3.0 Å, which is in agreement with the experimental determinations on solid MAN. The latter distance is also in agreement with the

Table 1. Average Distances and Angles Obtained for the Quantum Structures with wB97X-D[a]

compound	ionic couples	O···H distance (Å)	O···H–N angle (deg)
EAN	2	1.69	168.5
EAN	3	1.77	162.6
EAN	4	1.81	166.7
EAN	5	1.82	163.9
EAN	6	1.86	161.0
PAN	4	1.84	164.6
BAN	4	1.89	158.3
EAN	36	1.77	160.0
PAN	36	1.76	164.3
BAN	36	1.78	162.5

[a]Last lines: average distances obtained for a classical dynamics of 2 ns on a cluster of 36 ionic couples.

value reported in ref 37. As we noticed above, the classical simulations using the OPLS force field tend to produce a somewhat shorter O···H distance with respect to the ab initio DFT optimized structures.

In the DFT simulations of very small clusters, the average O···H distance is significantly smaller than the rest of the series, whereas it tends to increase by adding ionic couples. This is due to the natural tendency of the system to transfer the proton back from the base to the acid. As we reduce the number of ionic couples, the strength of the H-bond increases (and the H···O distance gets shorter) because the system "moves" toward the electronic configuration with no charge separation (neutralization reaction) which is, indeed, the ground state of the cluster with one ionic couple.

While H-bond geometric parameters are simply determined by ab initio gas-phase computations (as in this case) or by X-ray structural analysis, its energetic features are much more difficult to characterize[52,63] because H-bond shows a very high degree of energetic variations even in chemically similar system. In our case the H-bond is the result of an acid–base equilibrium or proton-transfer equilibrium RD–H +:AR′ ↔ RD^- + $^+$H–AR′. Its strength is fully controlled by the quantity $\Delta pK_a = pK[DH] - pK[AH^+]$.[63,64] Because in our case the $\Delta pK_a = pK_a[HNO_3] - pK_a[RNH_3^+] = -1.3 - 10.5 = -11.8$, the final H-bond will be a medium or weak one with a bent geometry and highly asymmetric A–H and D–H geometries. This model, in fact, perfectly suits the structural data reported in Table 1.

Despite these difficulties, it is still be possible to draw an energetic trend by looking at the variation of some key quantities versus the structure of the system. In particular, Ludwig and co-workers have shown[30,65] that there is a correlation between the low intramolecular vibrational frequencies due to H-bonding stretching motions, the binding energy of the ionic couple and the donor–acceptor delocalization energy ($E(2)$)[61] that can be calculated by a natural bond orbital (NBO) analysis of the ab initio wave function. This approach has been used to characterize the weak H-bonds that appear in nonprotic ionic liquids based on imidazolium moieties.[66] As far as we know, only one protic ionic liquid, PAN, has been studied by means of the above methods.[65] In that work the authors find a binding energy per ionic couples of 124.1 kcal and assign two broad FTIR absorption bands corresponding to H-bond stretching motions around 154 and 220 cm^{-1}. Although our experimental spectra do not provide that region of the spectra, we have identified

similar bands in all the theoretical spectra for the calculated clusters at very similar frequencies.

We report our calculated binding energies $\Delta E/n$, the delocalization energies $E(2)$ in Table 2. $E(2)$ is the sum of all the perturbative energies associated with the Fock operator elements between the oxygen lone pairs and the σ^* orbitals of the N−H in the NBO representation. The binding energy $\Delta E/n$ is the average ionic couple interaction energy in the cluster, at its fixed geometry calculated through a counterpoise procedure, i.e.:

Table 2. Energetic Features of the Reported Cluster Calculation: Delocalization and Binding Energies (All Values in kcal; Details in Text)

compound	ionic couples	$E(2)/n$	$\Delta E/n$
EAN	2	−76.6	−133.0
EAN	3	−64.2	−135.1
EAN	4	−58.5	−140.6
EAN	5	−66.5	−141.5
EAN	6	−64.8	−144.2
PAN	6	−70.9	−141.6
BAN	6	−71.0	−141.5

$$\Delta E = E[\text{cluster}] - \sum_{i=1}^{\text{no. of couples}} (E[\text{cation}_i] + E[\text{anion}_i]) \quad (1)$$

where all the energies are calculated in the "complete basis set".

The interaction energy per ionic couple has an almost constant value as a function of the cluster growth. We see, however, a small drift toward larger values that can be attributed, probably, to many body effects (in terms of molecular entities). On the other hand, the $E(2)/n$ value is seen to oscillate as the cluster grows, its precise value depending on the geometric configuration and representing around 40−45% of the binding energy. Each single H-bond actually has a much lower energy than the reported $E(2)$ value because each $[RNH_3^+][NO_3^-]$ complex is able to form more than one H-bond at the same time. By looking in more detail at the NBO analysis, we find the following:

- By locating the major contributions to $E(2)$ in each EAN cluster and for each pair of orbitals involved, it is possible to identify (both geometrically and energetically) a few "strong" H-bonds for which the delocalization energy $E(2)$ exceeds 10 kcal.
- These "strong" H-bonds are roughly twice the number of ionic couples showing that, at least in such clusters, the H-bond network is highly unsaturated, leading to each nitrate ion to form around 2 rather strong H-bonds out of the possible three (see below for a description of the consequences that this effect may have on the experimental Raman spectra).
- The cluster with $n = 4$ is an exception as it presents 12 strong $E(2)$ interactions owing to the peculiar symmetry of this species.
- Because the $E(2)$ represents a sort of upper limit to H-bond energy, we can therefore estimate the energy of these H-bonds, which turns out to range from 25 kcal for the $n = 2$ species to 15 kcal for the species with $n = 6$.
- In the PAN and BAN clusters the $E(2)$ energy turned out to be slightly larger than that we have found for EAN. Nevertheless, also the number of strong hydrogen bonds (i.e., those with $E(2) > 10$ kcal) was larger, thereby leading to a similar H-bond strength.

Raman Spectra. The collected spectra are reported in Figure 5 together with the theoretical spectra for the cluster with 4 ionic couples for the three compounds: EAN, PAN, and BAN. We have obtained very similar spectra for the clusters with 6 ionic couples and for EAN also for the cluster with 8 ionic couples although the latter has been treated at the B3LYP level for testing purposes. Anyway, most of the spectral features are almost independent from the aggregation number except for minor details. The simulated theoretical frequencies have

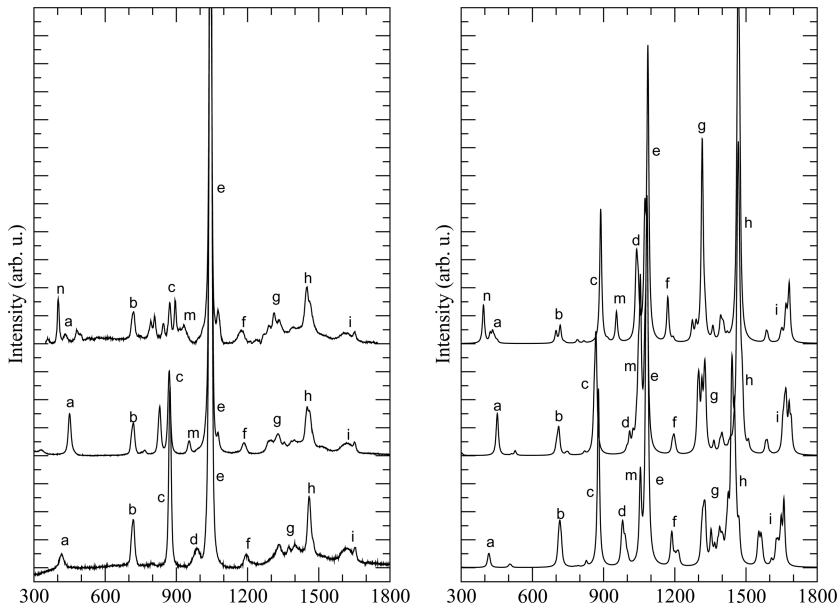

Figure 5. Left panel: experimental Raman spectra of liquid EAN, PAN, and BAN (from bottom to top). Right panel: theoretical spectra in the harmonic approximation for the clusters of EAN, PAN, and BAN with 4 ionic couples. The theoretical frequencies have been scaled by 0.96 to account for anharmonicity. The abscissa are wavenumbers in cm^{-1}.

dx.doi.org/10.1021/jp3052714 | J. Phys. Chem. B 2012, 116, 13878−13888

been scaled by 0.96 to account for anharmonicity. The band shape has been obtained by simply using a Gaussian line shape of 5 cm^{-1} width. The two sets of data show an excellent agreement in terms of peaks positions, thus allowing a careful assignment through the comparison with the ab initio spectra. Peak intensities for a given sample have been normalized to the height of the a peak (see in the following) to allow for a comparison between the measured and calculated spectra. Selected group of frequencies are also reported in Table 3 in numerical form.

Table 3. Theoretical and Experimental Frequencies of the Liquid and 4 Ionic Couples Clusters Respectively (Line Letters in Figure 5)

	expt freq (cm^{-1})			theor freq (cm^{-1} × 0.96)		
line	EAN	PAN	BAN	EAN	PAN	BAN
n			402			394
a	415	450	434	417	452	423–433
b	718	718	718	715	711	700–717
c	873	870	870–895	878	867	887
e	1044	1044	1044	1083	1082	1086
f	1195	1185	1174	1200	1196	1170
h	1460	1452	1450	1441	1467	1466

The first group labeled a at 416–450 cm^{-1} is due to C_n–N bending motions. In BAN we see the insurgence of another group of frequencies labeled *n* at lower frequencies that correspond to C_n–N concerted bending that leads to chain elongation, a motion that is not possible for shorter chains. The b group at 720 cm^{-1} is due to bending of the NO_3^- and the c peak is due to C_n–N symmetric stretching and lies at 870–890 cm^{-1}. In that region we find the frequencies typical of the pyramidal motion of the anion (825–830 cm^{-1}), but it is also likely that the more asymmetric chemical surroundings of the liquid phase with respect to our 4 couple cluster may lead to a proliferation of the C–C and C–N stretching motions frequencies.

The peaks labeled d are due to wagging motions of the CH_2 and CH_3 groups. The peak labeled m is due to asymmetric C–C and C–N stretching motions in the alkyl chains. The e peak around 1045 cm^{-1} is the NO_3^- symmetric stretching motion. The f group around 1175–1195 cm^{-1} is due to rocking motions of the CH_n groups. The g group of peaks is composed of many complex motions which are, however, all due to CH_n scissoring. In between this group, it is possible to find also the asymmetric stretching of NO_3^- around 1400–1420 cm^{-1}. The h group of peaks is due to the CH_2 and CH_3 bending motion. Peaks i are due to NH_3^+ scissoring/rocking motions.

Generally speaking, the lengthening of the alkyl chain leads to frequency shift of most of the experimental Raman peaks, which is well reproduced by the theoretical results. For example, the experimental trend shown by the a band is coherent with the theoretical one, it goes from 415 to 450 and to 434 cm^{-1} on lengthening the alkyl chain (i.e., going from EAN to PAN to BAN). A similar agreement between experiment and calculation is also shown by the f peak, which moves toward lower frequency on lengthening the alkyl chain (from 1195 to 1185 to 1174 cm^{-1}), and by the h peak, which goes from 1460 to 1452 and to 1450 cm^{-1} from EAN to PAN and to BAN. We notice that the frequencies of peaks b and e, both related to the anion vibrational modes, are not affected by the lengthening of the alkyl chain, as it is well shown by both the experimental and the theoretical spectra. We notice that although the spectral intensities are bound to the liquid dynamics, missing in our DFT simulation, the theoretical/experimental comparison shows, at least in several cases, a fairly good agreement of the relative intensities among the peaks in a given compound as well as of the intensity evolution of a given peak on lengthening the alkyl chain. The experimental relative intensities among different peaks are indeed qualitatively reproduced by the calculation and notably the intensities of a, b, and c peaks show experimental and theoretical trends quite

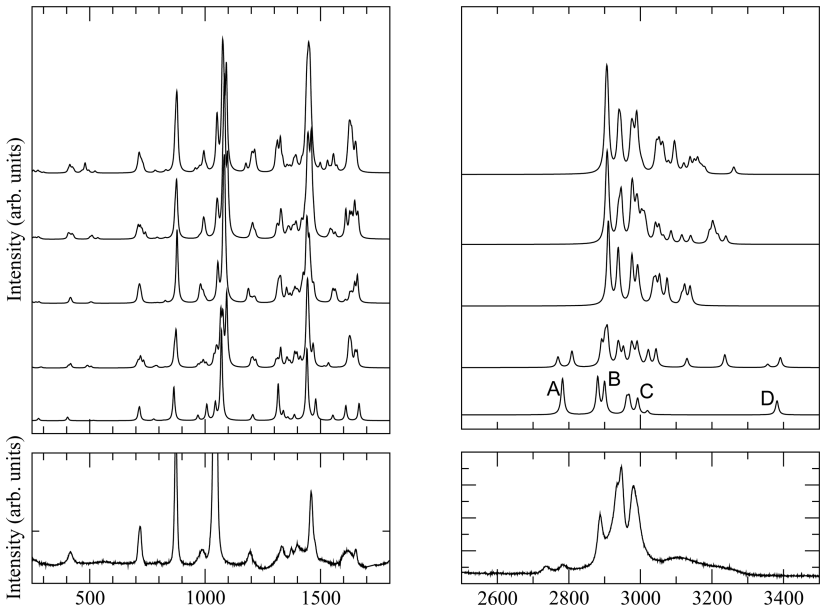

Figure 6. Lower panels: experimental Raman spectra of liquid EAN. Upper panels: theoretical spectra from bottom to top for the clusters with 2, 3, 4, 5, and 6 ionic couples. The theoretical frequencies have been scaled by 0.96 (right panel) and 0.95 (left one) to account for anharmonicity. The abscissa are wavenumbers in cm^{-1}.

dx.doi.org/10.1021/jp3052714 | J. Phys. Chem. B 2012, 116, 13878–13888

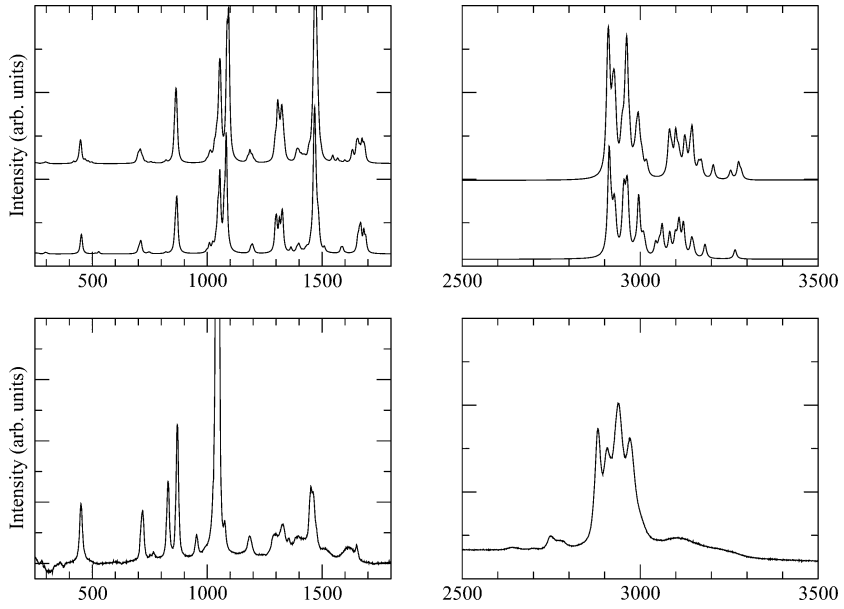

Figure 7. Lower panels: experimental Raman spectra of liquid PAN. Upper panels: theoretical spectra in the harmonic approximation for the cluster with 4 ionic couples (lower one) and 6 ionic couples (upper one). The theoretical frequencies have been scaled by 0.96 (low frequencies) and 0.95 (high frequencies) to account for anharmonicity. The abscissa are wavenumbers in cm^{-1}.

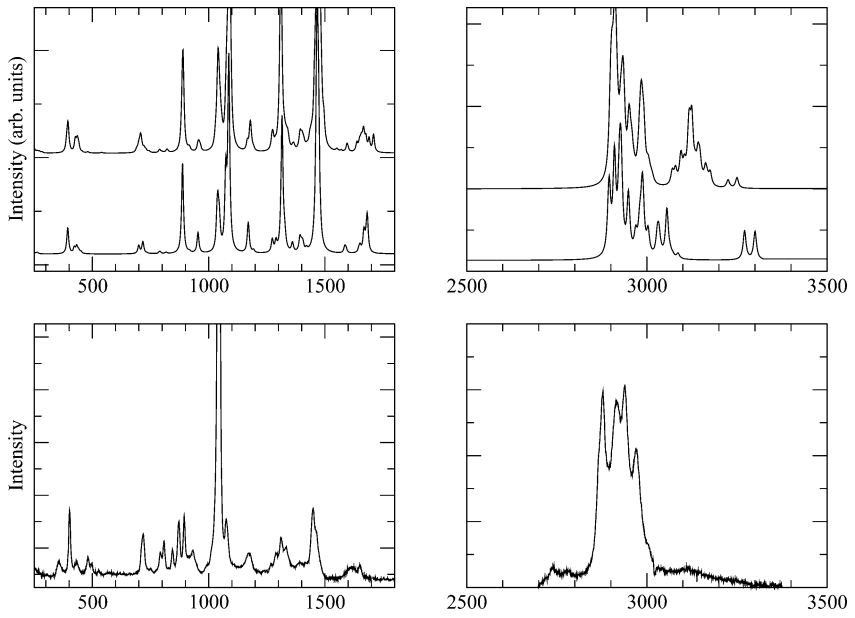

Figure 8. Lower panels: experimental Raman spectra of liquid BAN. Upper panels: theoretical spectra in the harmonic approximation for the cluster with 4 ionic couples (lower one) and 6 ionic couples (upper one). The theoretical frequencies have been scaled by 0.96 (low frequencies) and 0.95 (high frequencies) to account for anharmonicity. The abscissa are wavenumbers in cm^{-1}.

similar on going from EAN to BAN. For all the three spectra the h band is too intense in the DFT calculations with respect to the measured spectra; vice versa, the e band is less intense in the DFT spectra.

The liquid EAN Raman spectra compared with those obtained by DFT calculations are further reported in Figure 6. The simulated theoretical frequencies have been scaled by 0.96 (low frequencies) and 0.95 (high frequencies) to account for anharmonicity. We present here the theoretical spectra for an increasing number of ionic couples composing the cluster and also the high-frequency part of the spectrum. In the low-frequency range, the increase of the number of ionic couples does not enhance the spectral complexity and the intramolecular peaks pattern retains clearly its structure, which is well representative of the liquid experimental spectra. The high-frequency region, characterized by the presence of the C−H and N−H stretching peaks, shows instead clear progressive modifications when the number of possible H-bonds inside the cluster (i.e., the number of ionic couples) increases. In the case of two ionic couples cluster (bottom of the upper panels), we clearly see 4 groups of frequencies. The first one, A, is due to N−H motions involved in very strong H-bonds and that disappears when the cluster size increases and only barely survives in the one with 3 ionic couples. Two peaks at the same location are clearly visible in the measured spectra and although in the real liquid there may be a sizable fraction of very strong

dx.doi.org/10.1021/jp3052714 | J. Phys. Chem. B 2012, 116, 13878−13888

H-bonds, we cannot exclude the possibility that these bands are overtones. The B group consists of two peaks, the first one is due to N−H still involved in H-bonds, but whose bonding feature is weaker with respect to the A group, the second peak is due to the C−H stretching motions. The third band, C, is due to C−H motions, and finally, the D band, at 3390 cm^{-1}, is due to an N−H stretching motion that is not involved in H-bond.

The D spectral feature moves to lower frequencies when the cluster size increases (Figure 6), due to a progressive involvement of the N−H terminals in H-bonds. A sizable tail of frequencies is clearly visible between 3100 and 3250 cm^{-1} in both experiments and theory. This signals are obviously due to N−H stretching motions that are involved in weaker H-bonds with respect to those that produce the signal at 2900 cm^{-1} (B peak). This means that in the real liquid, as happens for the large clusters, there is, probably, a mixture of different H bonds strength so that the signals due to the N−H stretching are spread over a large range of frequencies from 2900 to 3300 cm^{-1}. The coexistence of a range of different H-bonding features is not unlike what we have already found in a study of solid phases of the MAN compound,[49] where two different H-bonds exists in the crystal, and what has been found in liquid MAN by Kirchner and co-workers in ref 47 where they argue the presence of a rather complex H-bonding network that, unlike water, presents an "unsaturated" acceptor−donor combination (i.e., one out of three possible acceptor is not involved in an H-bond).

In Figures 7 and 8 we report the spectra of PAN and BAN in the same fashion as we did for EAN, although now we limit the discussion to the spectra with 4 and 6 ionic couples. By comparison, we can readily see that the assignment of the resonant bands is almost exactly the same. The minor differences that clearly arise at high frequencies are due to the slightly different H-bonding networks in the two compounds. The finite size effect in the calculated clusters leads to the "freeing" of some of the N−H donors and therefore high-frequency N−H spectral features appear. In the experimental spectra the analogous effect of a coexistence of strong and weak H-bonds might be represented by the large and unstructured band that can be found at 3100−3200 cm^{-1}.

■ CONCLUSIONS AND PERSPECTIVES

We have performed several calculations both using a classical force field approach and a high-quality quantum DFT method to unravel the microscopic structure that characterize a special class of ionic liquids: *n*-alkylammonium nitrates. We have used the Raman spectra of the corresponding pure liquids as a guide to check the consistency of our calculations. The comparison between the calculated and measured spectra has turned out to be remarkably good in the fingerprint region whereas it is slightly less accurate in the high-frequency region. The differences between the cluster model and the measurements in the high-frequency region, far from being a signal of a poor modeling, have allowed us to trace interesting conclusions about the nature of the H-bonding interaction. More generally, the careful analysis of the spectra outlined in the present work has allowed us to produce evidence of the following structural features:

These ionic liquids have a very disordered microscopic structure[34] that is due to two driving forces: the coexistence of polar and apolar domain in the molecule and an asymmetric H-bonding network. The presence of an apolar alkyl chain prevents the formation a simple and ordered crystal structure and makes these substances liquids at mild conditions or even at room temperature (by contrast ammonium nitrate melts around 450 K). This effect is evident if we consider the lack of a simple geometrical structure even in an extremely small portion of the liquid such as the clusters of few ionic couples that we have presented above. Except for the structure with 4 ionic couples that seems to provide a rather distorted cubic-like arrangement of the H-bonds, the clusters with 6 or 8 ionic couples already show a high degree of structural disorder.

The second mechanisms that provide additional disorder in these systems is represented by the fact that, locally, the acceptor−donor network of H-bonds is incomplete or at least highly asymmetrical. In particular, we have noticed that, in the computed clusters, some of the nitrate anions tend to form only two H-bonds leaving one of their acceptor sites almost free. This, together with the finite size effect, leads to a dispersion of the N−H stretching vibrational frequencies in the calculated clusters between 2800 and 3400 cm^{-1}. This dispersion is indeed also present in the experimental spectra (though in a slightly more limited fashion), thereby pointing to a sort of unsaturation effect of the H-bonding network in the "real" liquid.

Such an effect has been also confirmed by an NBO perturbative analysis of the delocalization energy. We have shown that the total attractive contribution of the delocalization energy can be estimated to be roughly 40−50% of the total binding energy. We have also estimated that the binding energy due to a single H-bond in the computed clusters has an upper value ranging from 25 to 15 kcal depending on the size of the cluster and on the compound with the EAN $n = 2$ cluster showing the strongest binding. These values are in agreement with what has been recently found by Fumino et al. in ref 67. The NBO analysis has further confirmed that, for EAN, roughly only 2 out of 3 oxygen atoms of the nitrate ion are involved in strong H-bonds.

Alkyl chain elongation does not seem to produce a sizable effect on the H-bonding feature, at least by looking at the results at our level of calculation. In contrast, the general liquid structure is certainly affected and the relevant region of the Raman spectra (mainly the fingerprint one) clearly sees substantial changes among the three compounds. These changes have been identified mainly in the region of the C−N/C−C stretching motions and the C−C−N bending region.

An additional novelty of the present study is the fact that our cluster model predicts an acceptor−donor distance of 2.9 Å that is typical of a medium strength H-bond coming from the acid−base reaction O−H···N → O^-···H−N^+.[53] Despite the larger values estimated by recent MD calculations (see ref 38), the average H-acceptor distance, in the present cluster model, turns out to be of 1.9 Å, which is in line with the available data on N−H···O systems.[53]

■ AUTHOR INFORMATION

Corresponding Author

*E-mail: enrico.bodo@uniroma1.it.

Present Address

[‖]Department of Chemistry, University of Rome "La Sapienza", P. A. Moro 5, 00185, Rome, Italy.

Notes

The authors declare no competing financial interest.

■ ACKNOWLEDGMENTS

Financial support of the Scientific Committee of the University of Rome and of the PRIN national project n. 2009WHPHRH_001 is gratefully acknowledged. Computational support of the CASPUR (grants std11-424) and CINECA (grant IscraB_ASIL) Supercomputing Centers is also acknowledged. This work has been conceived and developed within the Ionic Liquids group of the University of Rome "La Sapienza", which is therefore acknowledged for the useful discussions and valuable suggestions.

■ REFERENCES

(1) Rogers, R. D., Seddon, K. R., Eds. *Ionic Liquids IIIA: Fundamentals, Progress, Challenges, and Opportunities: Properties and Structure*; ACS Symposium Series; American Chemical Society: Washington, D.C., 2005; Vol. *901*; p 356.
(2) Rogers, R., Seddon, K., Eds. *Ionic Liquids IIIB: Fundamentals, Progress, Challenges, and Opportunities: Transformations and Processes*; ACS Symposium Series; American Chemical Society: Washington, D.C., 2005; Vol. *902*.
(3) Rogers, R. D., Plechkova, N. V., Seddon, K. R., Eds. *Ionic Liquids: From Knowledge to Application*; ACS Symposium Series; American Chemical Society: Washington, D.C., 2009; Vol. *1030*; p 464.
(4) Gaune-Escard, M., Seddon, K. R., Eds. *Molten Salts and Ionic Liquids: Never the Twain?*; Wiley: New York, 2010; p 441.
(5) Walden, P. *Bull Acad. Imper. Sci. (St Petersburg)* **1914**, 1800.
(6) Plechkova, N. V.; Seddon, K. R. *Chem. Soc. Rev.* **2008**, *37*, 123–150.
(7) Welton, T.; ,Wasserscheid, P., Eds. *Ionic Liquid Synthesis*, 2nd ed.; Wiley VCH: Weinheim, 2008; p 721.
(8) Stark, A.; Seddon, K. R. In *Kirk-Othmer Encyclopaedia of Chemical Technology*, 5th ed.; Seidel, A., Ed.; John Wiley & Sons, Inc.: Hoboken, NJ, 2007; Vol. *26*, pp 836–920.
(9) Freemantle, M. *An Introduction to Ionic Liquids*; RSC Publishing: London, 2009; p 281.
(10) Forsyth, S. A.; Pringle, J. M.; MacFarlane, D. R. *Aust. J. Chem.* **2004**, *57*, 113–119.
(11) Zeng, Z.; Phillips, B. S.; Xiao, J.-C.; Shreeve, J. M. *Chem. Mater.* **2008**, *20*, 2719–2726.
(12) Hough, W. L.; Rogers, R. D. *Bull. Chem. Soc. Jpn.* **2007**, *80*, 2262–2269.
(13) Hough, W. L.; Smiglak, M.; Rodriguez, H.; Swatloski, R. P.; Spear, S. K.; Daly, D. T.; Pernak, J.; Grisel, J. E.; Carliss, R. D.; et al. *New J. Chem.* **2007**, *31*, 1429–1436.
(14) Mizuuchi, H.; Jaitely, V.; Murdan, S.; Florence, A. *Eur. J. Pharmac. Sci.* **2008**, *33*, 326.
(15) Boon, J. A.; Levisky, J. A.; Pflug, J. L.; Wilkes, J. S. *J. Org. Chem.* **1986**, *51*, 480–3.
(16) Fischer, T.; Sethi, A.; Welton, T.; Woolf, J. *Tetrahedron Lett.* **1999**, *40*, 793–796.
(17) Wasserscheid, P.; Keim, W. *Angew. Chem., Int. Ed.* **2000**, *39*, 3772–3789.
(18) Welton, T. *Chem. Rev.* **1999**, *99*, 2071–2083.
(19) Koel, M. *C. Rev. Ann. Chem.* **2005**, *35*, 177.
(20) Tan, S. S. Y.; MacFarlane, D. R.; Upfal, J.; Edye, L. A.; Doherty, W. O. S.; Patti, A. F.; Pringle, J. M.; Scott, J. L. *Green Chem.* **2009**, *11*, 339.
(21) Sun, H.; Zhang, D.; Liu, C.; Zhang, C. *THEOCHEM* **2009**, *900*, 37.
(22) Buzzeo, M. C.; Evans, R. G.; Compton, R. G. *ChemPhysChem* **2004**, *5*, 1106.
(23) Endres, F.; Abedin, S. Z. E. *Phys. Chem. Chem. Phys.* **2006**, *8*, 2101.
(24) Hapiot, P.; Lagrost, C. *Chem. Rev.* **2008**, *108*, 2238.
(25) MacFarlane, D. R.; Forsyth, M.; Howlett, P. C.; Pringle, J. M.; Sun, J.; Annat, G.; Neil, W.; Izgorodina, E. I. *Acc. Chem. Res.* **2007**, *40*, 1165.
(26) Angell, C. A.; Byrne, N.; Belieres, J.-P. *Acc. Chem. Res.* **2007**, *40*, 1228–1236.
(27) Greaves, T. L.; Drummond, C. J. *Chem. Rev.* **2008**, *108*, 206–237.
(28) Xu, W.; Angell, C. A. *Science* **2003**, *302*, 422–425.
(29) Yoshizawa, M.; Xu, W.; Angell, C. A. *J. Am. Chem. Soc.* **2003**, *125*, 15411–15419.
(30) Fumino, K.; Wulf, A.; Ludwig, R. *Angew. Chem., Int. Ed.* **2009**, *48*, 3184–3186.
(31) Emelýanenko, V. N.; Verevkin, S. P.; Heintz, A.; Voss, K.; Schulz, A. *J. Phys. Chem. B* **2009**, *113*, 9871–9876.
(32) Nakamoto, H.; Watanabe, M. *Chem. Commun.* **2007**, 2539–2541.
(33) Fumino, K.; Peppel, T.; Geppert-Rybczyńska, M.; Zaitsau, D. H.; Lehmann, J. K.; Verevkin, S. P.; Köckerling, M.; Ludwig, R. *Phys. Chem. Chem. Phys.* **2011**, *11*, 14064–14075.
(34) Atkin, R.; Warr, G. G. *J. Phys. Chem. B* **2008**, *112*, 4164–4166.
(35) Greaves, T. L.; Weerawardena, A.; Krodkiewska, I.; Drummond, C. J. *J. Phys. Chem. B* **2008**, *112*, 896–905.
(36) Mamontov, E.; Luo, H.; Dai, S. *J. Phys. Chem. B* **2009**, *113*, 159–169.
(37) Hayes, R.; Imberti, S.; Warr, G. G.; Atkin, R. *Phys. Chem. Chem. Phys.* **2011**, *13*, 3237–3247.
(38) Song, X.; Hamano, H.; Minofar, B.; Kanzaki, R.; Fujii, K.; Kameda, Y.; Kohara, S.; Watanabe, M.; Ishiguro, S.-i.; Umebayashi, Y. *J. Phys. Chem. B* **2012**, *116*, 2801–2813.
(39) Zahn, S.; Thar, J.; Kirchner, B. *J. Chem. Phys.* **2010**, *132*, 124506.
(40) Maginn, E. J. *J. Phys. Condens. Matter* **2009**, *21*, 373101.
(41) Canongia Lopes, J. N.; Deschamps, J.; Pádua, A. A. H. *ACS Symp. Ser.* **2005**, *901*, 134–149.
(42) Canongia Lopes, J. N. A.; Pádua, A. A. H. *J. Phys. Chem. B* **2006**, *110*, 7485–7489.
(43) Borodin, O. *J. Phys. Chem. B* **2009**, *113*, 11463–11478.
(44) Sambasivarao, S. V.; Acevedo, O. *J. Chem. Theory Comput.* **2009**, *5*, 1038–1050.
(45) Bodo, E.; Gontrani, L.; Triolo, A.; Caminiti, R. *J. Phys. Chem. Lett.* **2010**, *1*, 1095–1100.
(46) Bodo, E.; Gontrani, L.; Caminiti, R.; Plechkova, N. V.; Seddon, K. R.; Triolo, A. *J. Phys. Chem. B* **2010**, *114*, 16398.
(47) Zahn, S.; Thar, J.; Kirchner, B. *J. Chem. Phys.* **2010**, *132*, 124506.
(48) Izgorodina, E. I. *Phys. Chem. Chem. Phys.* **2011**, *13*, 4189–4207.
(49) Bodo, E.; Postorino, P.; Mangialardo, S.; Piacente, G.; Ramondo, F.; Bosi, F.; Ballirano, P.; Caminiti, R. *J. Phys. Chem. B* **2011**, *115*, 13149–13161.
(50) Hayes, R.; Imberti, S.; Warr, G. G.; Atkin, R. *Phys. Chem. Chem. Phys.* **2011**, *13*, 13544–13551.
(51) Jorgensen, W. L.; Maxwell, D. S.; Tirado-Rives, J. *J. Am. Chem. Soc.* **1996**, *117*, 11225–11236.
(52) Gilli, G.; Gilli, P. *The Nature of the Hydrogen Bond: Outline of a Comprehensive Hydrogen Bond Theory*;, 1st ed.; International Union of Crystallography Monographs on Crystallography; Oxford University Press: Oxford, U.K., 2009; p 336.
(53) Gilli, P.; Pretto, L.; Bertolasi, V.; Gilli, G. *Acc. Chem. Res.* **2009**, *42*, 33–44.
(54) Kennedy, D. F.; Drummond, C. J. *J. Phys. Chem. B* **2009**, *113*, 5690.
(55) Robert, C.; Casella, G. *Monte Carlo Statistical Methods*; Springer-Verlag: Berlin, 2004.
(56) Hartke, B. *J. Phys. Chem.* **1993**, *97*, 9973–9976.
(57) http://dasher.wustl.edu/tinker/.
(58) Lebrero, M. C. G.; Bikiel, D. E.; Elola, M. D.; Estrin, D. A.; Roitberg, A. E. *J. Chem. Phys.* **2002**, *117*, 2718–2725.
(59) Frisch, M. J.; et al. *Gaussian 09*, Revision A.1; Gaussian Inc.: Wallingford, CT, 2009.
(60) Chai, J.-D.; Head-Gordon, M. *Phys. Chem. Chem. Phys.* **2008**, *10*, 6615–6620.
(61) Reed, A. E.; Curtiss, L. A.; Weinhold, F. *Chem. Rev.* **1988**, *88*, 899–926.
(62) Zahn, S.; Kirchner, B. *J. Phys. Chem. A* **2008**, *112*, 8430–8435.

(63) Gilli, P.; Gilli, G. *J. Mol. Struct.* **2010**, *972*, 2−10.
(64) Gilli, P.; Gilli, G. *J. Mol. Struct.* **2007**, *844*−*845*, 328−339.
(65) Fumino, K.; Wulf, A.; Ludwig, R. *Phys. Chem. Chem. Phys.* **2009**, *11*, 8790−8794.
(66) Dong, K.; Song, Y.; Liu, X.; Cheng, W.; Yao, X.; Zhang, S. *J. Phys. Chem. B* **2012**, *116*, 1007.
(67) Fumino, K.; Reichert, E.; Wittler, K.; Hempelmann, R.; Ludwig, R. *Angew. Chem. Int. Ed.* **2012**, *51*, 6236−6240.